Flame suppression ability of metallocenes (nickelocene, cobaltocene, ferrocene, manganocene, and chromocene)

Yusuke Koshiba [a]*, Yohei Takahashi [b], Hideo Ohtani [c]

[a]Division of Materials Science and Chemical Engineering, Faculty of Engineering, Yokohama National University, 79-5 Tokiwadai, Hodogaya-ku, Yokohama, 240-8501, Japan

[b]Department of Risk Management and Environmental Sciences, Graduate School of Environment and Information Sciences, Yokohama National University, 79-7 Tokiwadai, Hodogaya-ku, Yokohama, 240-8501, Japan

[c]Division of Safety Management, Faculty of Environment and Information Sciences, Yokohama National University, 79-7 Tokiwadai, Hodogaya-ku, Yokohama, 240-8501, Japan

*Corresponding author: Telephone number: +81-45-339-3985

Fax number: +81-45-339-3985

E-mail address: ykoshiba@ynu.ac.jp

Complete postal address: 79-5 Tokiwadai, Hodogaya-ku, Yokohama 240-8501, Japan

Abstract

This article reports experimental investigation of flame suppression ability of metallocenes. In this study, chromocene ($CrCp_2$), manganocene ($MnCp_2$), ferrocene ($FeCp_2$), cobaltcene ($CoCp_2$), and nickelocene ($NiCp_2$) are used. The experiments are conducted by combusting a filter paper on which the metallocene is absorbed, by thermogravimetric measurement for metallocene/cellulose systems, and by burning a solution of the metallocene in n-pentane. Their suppression abilities are characterized with three parameters: extinction limit; activation energy of degradation; and burning rate of the liquid fuel. These experiments confirm that: (i) the metallocenes offer better flame suppression ability compared to ammonium dihydrogen phosphate, which is a conventional fire extinguishing agent; (ii) the metallocenes can exhibit the suppression effect not in solid phase but in gas phase; (iii) the suppression ability is in order of $CrCp_2 > MnCp_2 > FeCp_2 > CoCp_2 > NiCp_2$, i.e., the metallocenes are arranged in order of the atomic number of their central metal. Although the metallocenes (except $FeCp_2$) are chemically unstable, they are expected to be an excellent flame suppressant.

1. Introduction

Since a worldwide ban on the production of the catalytic fire extinguishing agent CF_3Br (Halon 1301), a number of studies have been reported on an alternative [1]. In particular, transition metal compounds such as iron, chromium, manganese, copper, and tin compounds have received much attention due to their strong radical-scavenging ability in flame chain reactions [2–4]. Among these metallic compounds, iron pentacarbonyl ($Fe(CO)_5$) is up to two orders of magnitude more effective than Halon 1301, indicating that it is an excellent flame inhibitor. A number of experimental and numerical studies have made clear the high suppression ability and inhibition mechanism of $Fe(CO)_5$ [5–9]. However, the use of $Fe(CO)_5$ as an extinguishing agent is not always practical because of its high inflammability and severe toxicity at high concentrations. In contrast, ferrocene ($FeCp_2$) in which the iron has the same coordination in $Fe(CO)_5$, is less toxic. Several studies have been reported on relatively high extinguishing ability of $FeCp_2$ [10–14].

Linteris et al. [15], and Babushok and Tsang [16] have compiled experimental results of the normalized flame inhibition abilities of many metallic and non-metallic compounds. Although the results may not be able to be directly compared, Fe-, Cr-, or Mn-containing compounds are most effective. Next to these transition metallic compounds, alkali metal compounds have better suppression ability. As would be expected from these results, compounds containing the transition metals are candidates for high-efficiency extinguishing agents.

Our previous paper [17] has showed that as far as iron compounds having ionic bonds are compared, there are relatively positive correlations between their extinguishing abilities and bond dissociation energies around the metal, i.e., an iron compound with a smaller bond dissociation energy shows a higher extinguishing ability. It is noteworthy that a metallocene has weak coordination bonds between the central metal and cyclopentadienyl ligands, exhibiting smaller bond dissociation energies compared to general inorganic salts. Although not all metallocenes are chemically stable, it is possible that some metallocenes exhibit better extinguishing abilities than $FeCp_2$. No systematic studies, however, have been reported on the inhibition effectiveness of metallocenes.

The focus of the present study is on experimental investigation of the basic flame-suppression ability of metallocenes. This study employs $FeCp_2$, manganocene ($MnCp_2$), nickelocene ($NiCp_2$), chromocene ($CrCp_2$), and cobaltocene ($CoCp_2$) as commercially available metallocenes. All the central metals are divalent cations.

In order to experimentally evaluate their suppression abilities, the experiments are conducted by combusting a filter paper on which the metallocene is absorbed, by thermogravimetric (TG) analysis, and by burning a solution of the metallocene in n-pentane. Flame-suppression behavior of the metallocenes is characterized with three parameters: flame-extinction limit (mol g^{-1}), activation energy of the cellulose degradation (kJ mol^{-1}), and burning rate of the solution (mm min^{-1}). A

comparison of the ability is made between the metallocenes and ammonium dihydrogen phosphate ($NH_4H_2PO_4$), which is a conventional extinguishing agent.

In general, the flame suppression effects of chemicals are difficult to directly compare when used with inorganic compounds having different types or numbers of counterion(s) because the suppression effect of the counterion(s) is observed simultaneously with that of the metal species. In contrast, the use of metallocenes provides an advantage that the experiments take the suppression effect of the counterion to be constant: the experiment allows direct comparison of the extinguishing abilities among these metallocenes.

2. Material and methods

2.1 Chemicals and materials

$NiCp_2$, $CoCp_2$, and $FeCp_2$ were purchased from Wako Pure Chemical Industries, Ltd. (Osaka, Japan). $MnCp_2$ and $CrCp_2$ were obtained from Strem Chemicals, Inc. (Newburyport, MA, USA) and Mitsuwa Chemicals Co., Ltd. (Osaka, Japan), respectively. All these metallocenes were of reagent grade. The purity of all the metallocenes other than $NiCp_2$ is > 98%; $NiCp_2$ has a purity of > 95%. The chemical structures of the metallocenes are depicted in Fig. 1. A filter paper with a uniform thickness of 0.18 mm and a density of 87 g m^{-2} was purchased from Toyo Roshi Kaisha, Ltd. (Tokyo, Japan). All solvents and fuels were treated over molecular sieves to remove a trace amount of

water.

2.2 Filter-paper fires

This experiment employs the filter paper made from natural cellulose as a typical combustible solid. The filter paper was cut into strip-shaped papers with dimensions of 100.0 mm in length by 5.0 mm in width using a PTFE (polytetrafluoroethylene) cutter in order to avoid influence of a small amount of metal powders. The strip-shaped paper was dried in a vacuum desiccator for 48 h, and then its weight was measured. The paper was immersed into a solution of the metallocene in toluene. After the immersion, the paper was taken out and subsequently dried in the desiccator for 48 h, making the specimens apparently homogeneous.

In this study, the absorption concentration of the suppressant, C_S (mol g^{-1}), on the specimen is defined as Eq. (1).

$$C_S = (W_S / W_P - 1) / M_M \qquad (1)$$

where W_S is the weight of the specimen: the weight of the strip-shaped paper on which the suppressant is absorbed, W_P is the mass of only the dry strip-shaped paper, and M_M is molecular weight of the suppressant (the metallocene or $NH_4H_2PO_4$). The concentration C_S is defined as the

number of moles of the suppressant per unit weight of the filter paper.

Fig. 2 illustrates schematic diagram of the experimental apparatus to observe behavior of flame over the specimen. The apparatus consists of an acrylic tube, a current plate, a mass flow contoller, and a specimen folder. The tube measures 300 mm in height by 80 mm in diameter. Dry air was passed at a flow rate of 5.0 L min^{-1} via the mass flow contollerand the current plate. The air flow enters from the bottom and exits from the top. We confirmed that the air flow was laminar.

The top of the specimen was ignited with a pilot flame, and then flame spread rate of the specimen was determined by measuring the time during which the flame spread down from 10 mm to 80 mm from the top of specimen, i.e., the time required to spread by 70 mm was measured. The reason why the experiment ignored the initial flame spreading of 10 mm is to avoid the influence of the pilot flame.

The flame suppression ability here is investigated by measuring the extinction limit of the metallocene.

2.3 Thermogravimetric measurements

Thermogravimetric experiments were carried out to observe the extinction ability of the metallocene in solid phase. The thermogravimetric measurements were performed on a Shimadzu TGA–50 thermogravimetric analyzer (Kyoto, Japan). The temperature calibration of the instrument

was conducted with pure standards of indium, tin and zinc.

Specimens composed of the filter paper and the metallocene for the thermogravimetric experiment were prepared in the same way as in Section 2.2. The specimen was cut finely, and then dried in a vacuum desiccator for 48 h. A clean aluminum or alumina crucible was charged with 5.0 mg of the specimen. The TG curves were obtained under an air atmosphere with the flow rate of 50 mL min^{-1}, applying at heating rates of 5, 10, and 20 K min^{-1} over the temperature range of room temperature to 873 K.

2.4 Pool fires

This experiment was conducted to observe the flame suppression ability of the metallocene in gas phase using n-pentane pool fire. n-Pentane was used as a fuel instead of n-heptane, which is a commonly-used reference fuel, because of low solubility of the metallocene in n-heptane.

A solution of the metallocene in n-pentane was prepared with its concentration of 10, 50, 100, and 200 ppm (mass/mass). Here the concentration of 200 ppm means a saturation point of $MnCp_2$ having lowest solubility among the metallocene used. A glass pan with dimensions of 30 mm in diameter and 10 mm in depth was placed on a thermal insulation plate, and then charged with the solution (5.0 mL). Burning rates of the solutions (mm min^{-1}) were measured. Fig. 3 shows the simplified diagram of the experimental apparatus.

3. Results

3.1 Filter paper fires

This experiment evaluates the metallocene for their flame suppression abilities using extinction limit and downward flame spread rate. Normalized flame spread rate, V, is expressed as Eq. (2).

$$V = U / U_0 \qquad (2)$$

where U_0 (mm sec^{-1}) is flame spread rate of only the strip-shaped paper, and U (mm sec^{-1}) is the rate of the sample.

In general, most organic polymers such as native cellulose combust with flame. This is because the heated polymer decomposes or breaks down to combustible gases above its decomposition temperature, generating a diffusion flame over the polymer. In such the situation, the downward flame spread rate of a thin flammable polymer is known to be steady under given conditions [18].

In Fig. 4, the normalized flame spread rate is plotted against concentration of the flame suppressant in the specimen. Fig. 4a shows the effect of $NH_4H_2PO_4$ concentration on the normalized flame spread rate. The flame spread rate decreased gradually with increasing the concentration at relatively low concentrations, and then decreased steeply over about 4×10^{-4} mol g^{-1}. The extinction

limit of $NH_4H_2PO_4$ was determined to be 5.25×10^{-4} mol g^{-1}.

Their flame suppression behaviors are shown in Fig. 4b and c, respectively. The flame suppression behaviors of $NiCp_2$ and $CoCp_2$ were very similar: even with a large amount of the metallocene on the specimen, these metallocenes did not result in the extinction of the flame. Interestingly, the normalized flame spread rate increased again above a certain concentration. This behavior reflects a bilateral character of these metallocenes: inflammability and flame-suppression ability. In relatively higher concentrations, inflammability of the metallocenes themselves exceeds the extinction effect of the metal species, resulting in the observed behavior.

Fig. 4d shows the variation in the flame spread rate as a function of the concentration of $FeCp_2$. The significant difference in the suppression behavior was found between $FeCp_2$ and the flame suppressants mentioned above ($NiCp_2$, $CoCp_2$, and $NH_4H_2PO_4$). In low concentrations, the normalized flame spread rate decreased dramatically with an increase in the concentration of $FeCp_2$ with a slope of 2.0×10^4 g mol^{-1}. Glowing was observed over the concentration range of 0.10×10^{-4} to 0.50×10^{-4} mol g^{-1}. The normalized flame spread rate reached zero in the concentration range of 0.50×10^{-4} to 9.00×10^{-4} mol g^{-1}, i.e. $FeCp_2$ had an extinction limit of 0.50×10^{-4} mol g^{-1}. This value is smaller by a factor of 11 than the extinction limit of $NH_4H_2PO_4$, allowing it to act as a good flame suppressant. However, similarly to $NiCp_2$ and $CoCp_2$, the flame spread rate increased again under high $FeCp_2$ concentration conditions. This result indicates that control of amount of $FeCp_2$ is of

practical importance when $FeCp_2$ is added to a flame.

Fig. 4e and f illustrates the flame suppression behavior of $MnCp_2$ and $CrCp_2$, respectively. The insets display expanded plots in lower concentrations of the metallocene. $MnCp_2$ and $CrCp_2$ exhibit a better flame-suppression ability compared to not only $NH_4H_2PO_4$ but also $FeCp_2$. In lower concentrations, $MnCp_2$ and $CrCp_2$ made it possible to dramatically decrease the normalized flame spread rate with the slope of 14.3 g mol^{-1}, and 6.7 g mol^{-1}, respectively. In addition, the initiation concentration of the glowing was 0.02 mol g^{-1}. Since $MnCp_2$ and $CrCp_2$ have an absorption limit beyond which the specimen with a uniform absorption of the metallocene cannot be prepared in low concentrations, the normalized flame spread rate did not increase again.

Table 1 summarizes the absorption limits, the initiation concentrations of glowing, and the extinction limits of these metallocenes and $NH_4H_2PO_4$. Comparisons of the results reveal that the extinction limit of $MnCp_2$ and $CrCp_2$ is smaller by a factor of 35 and 75, respectively, compared to that of $NH_4H_2PO_4$. Moreover, it is clear that the flame suppression ability is in order $CrCp_2 > MnCp_2 > FeCp_2 > CoCp_2 > NiCp_2$, showing that the metallocenes are arranged in order of the atomic number of their central metal. This is because the flame suppression ability depends strongly on the mole fraction of the inhibiting species in the gas phase at the flame. Hence, estimation of the mole fraction is of great importance for evaluating their suppression effectiveness and the ranking of the metals' suppression ability. However, we do not refer to their accurate mole fractions in gas phase

here because the concentration of the metallocene was used in this study.

All the metallocenes used in this study (except $FeCp_2$) are known to be unstable in a humid environment, and tend to decompose easily. Thus, the effects of the degradation on their flame suppression capabilities need to be investigated. A specimen with a $MnCp_2$ concentration of 0.15 $\times10^{-4}$ mol g^{-1}, one with a $CrCp_2$ concentration of 0.07 $\times10^{-4}$ mol g^{-1}, and one with a $FeCp_2$ concentration of 0.50×10^{-4} mol g^{-1} were prepared. As mentioned above, these values relate to the extinction concentrations of each compound. Fig. 5a shows the flame suppression ability of the specimens stored in humid air under light-shielding conditions. In the figure, the normalized flame spread rate is plotted against the storage time (τ). Naturally enough, use of these metallocenes allows extinction of the flame when $\tau = 0$ h. With $FeCp_2$, no remarkable increase in the normalized flame spread rate was observed during testing, indicating that $FeCp_2$ was hardly influenced by humidity. In contrast, in the case of $MnCp_2$ and $CrCp_2$, these normalized flame spread rates increased as the storage time increased. By comparing $MnCp_2$ with $CrCp_2$, it is clear that the slope of $MnCp_2$ was larger than that of $CrCp_2$, indicating that humidity had a stronger degradation effect on $MnCp_2$ than $CrCp_2$.

A comparison of a specimen stored in a drying environment with the above-mentioned specimen placed in the humid atmosphere permits discussion of humidity effects. The results revealed that: (i) there was little difference in the slope between $MnCp_2$ and $CrCp_2$ (see Fig. 5b); (ii) the normalized

flame spread rate of $FeCp_2$ remained unchanged and unaffected; and (iii) the specimen stored in a desiccator had a gentler slope compared to the specimen put in the humid environment. Even when the specimen with $MnCp_2$ or $CrCp_2$ was set under dry and light-shielding environments, the normalized flame spread rate was gradually enhanced with τ, implying that oxygen might affect the degradation. The experiments confirmed a problem regarding the long-term storage of these chemicals. This is due to the inherent instability of the metallocenes.

3.2 Thermogravimetric analysis

In Section 3.1, the flame suppression ability of the metallocene was evaluated by measuring the flame spread rate of the metallocene/cellulose system. This section deals with TG analysis in order to examine the metallocene/cellulose system for fundamental mass-change behavior. The TG analysis can provide insight into the suppression mechanism of the metallocene for cellulose, i.e., the TG experiments can make clear the phase in which the metallocene exhibits the suppression ability.

The TG measurement requires that a crucible material does not have catalytic effects for the specimen and its decomposition gases. In general, a crucible made of aluminum, alumina, platinum, or quartz is used. This study employs both the aluminum and alumina crucibles for the TG measurements in order to investigate the influence of the crucible material on thermal behavior of the specimens. As a result, there was no obvious difference in the catalytic effect on the mass-change

behavior between the aluminum crucible and alumina crucible. Hereafter this article contains the experimental results for the case where the aluminum crucible was used.

In all metallocenes, the TG measurements revealed that a single mass change step was observed. The mass loss associated with the loss of water was not found, reflecting the sufficient drying of the specimen. As an example of the TG analysis, TG and the derivative (DTG) curves of $MnCp_2$ are shown in Fig. 6.

The TG results of the metallocenes such as onset temperature ($T_{onset, M}$), temperature at the maximum of mass change for reaction ($T_{max, M}$), and residual mass (RM_M) at 873 K are summarized in Table 2. The onset temperatures of $NiCp_2$, $CoCp_2$, $FeCp_2$, $MnCp_2$, and $CrCp_2$ were found to be 381 K, 378 K, 376 K, 375 K, and 373 K, respectively. The residual mass of the specimen reached about zero by 423 K. These temperatures are so low that the metallocene easily breaks down in the flame, enabling it to introduce the flame-suppressant species (e.g. the metallic atom) into the flame. In addition, the results reveal that the ease with which the reaction occurs was in the order of $CrCp_2$ > $MnCp_2$ > $FeCp_2$ > $CoCp_2$ > $NiCp_2$, i.e., the metallocenes are arranged in order of the atomic number of their central metal.

In order to make clear the influence of the metallocene on cellulose, cellulose mixed with the metallocene was examined for mass-change behavior. Here we let the metallocene concentrations be at their extinction limits presented in Section 3.1: the $FeCp_2$, $MnCp_2$, and $CrCp_2$ concentrations were

set to 5.00×10^{-5} mol g^{-1}, 1.50×10^{-5} mol g^{-1}, and 0.70×10^{-5} mol g^{-1}, respectively. Since NiCp$_2$

and CoCp$_2$ were not able to extinguish the flame, the concentrations of NiCp$_2$ and CoCp$_2$ were

chosen to be 5.00×10^{-4} mol g^{-1}. The value relates to their lowest flame spread rates. As an example

of the TG analysis, TG and the DTG curves of MnCp$_2$ are depicted in Fig. 7. The TG measurement

demonstrated the mass loss of the specimen at three stages: the first mass loss at about 325 K is due

to removal of water from cellulose, the second one corresponds to the thermal reaction of the

metallocene involving mass loss, and the third one at about 630 K results from thermal reaction or

degradation of cellulose. Our measurements confirmed that other metallocene/cellulose specimens

showed similar mass-loss behavior to the MnCp$_2$/cellulose specimen.

The onset temperature of cellulose ($T_{onset, c}$), temperature at the maximum of mass change of

cellulose ($T_{max, c}$), residual mass (RM_c) at 873 K are summarized in Table 3. The results showed that:

(i) there was no significant difference in the onset temperatures among the specimens; (ii) addition

of the metallocene was not able to change the onset temperature of cellulose; and (iii) although

addition of the metallocene somewhat affected the residual mass, there was no significant tendency.

We calculated apparent activation energies of the specimens relating to the degradation of

cellulose in order to quantitatively evaluate the influence of the metallocene on the reaction. The

activation energy is calculated using Kissinger method (Eq. 3) [19].

$$\ln \left(\beta/T^2_{\max}\right) = -E_a/RT_{\max} + \text{Const.} \qquad (3)$$

where β is heating rate ($\beta = dT/dt$), E_a is activation energy, and R is the gas constant. The Kissinger

method has been used to calculate the activation energy in many studies [20, 21]. Plotting of

$\ln(\beta/T^2_{\max})$ against ($1/T_{\max}$) gives the activation energy E_a from the slope.

As an example, the Kissinger plot of the cellulose/MnCp$_2$ specimen is shown in Fig. 8. In all the

cellulose/metallocene specimens, we confirmed that the curve fit was quite good, with a correlation

coefficient of > 0.98. The activation energy E_a can be determined by calculating the slop of the line

following Eq. (3). The results of the apparent activation energies are listed in Table 4. The activation

energies of cellulose with NiCp$_2$, CoCp$_2$, FeCp$_2$, MnCp$_2$, and CrCp$_2$ were calculated to be 347 kJ

mol^{-1}, 349 kJ mol^{-1}, 346 kJ mol^{-1}, 345 kJ mol^{-1}, and 347 kJ mol^{-1}, respectively. The results reveal

that: (i) no clear differences in the activation energies were observed; and (ii) these values were

comparable to the activation energy of only cellulose determined by the same method (348 kJ mol^{-1}).

In other words the metallocenes tested hardly influenced the combustion kinetics of cellulose in the

metallocene concentration range. The metallocenes cannot exhibit the suppression effect in the solid

phase.

3.3 Pool fires

In general, the effect of fire suppressants in gas phase has been investigated by introduction of a suppressant into burner flame [22]. However, since all the metallocenes used in this study are insoluble in water, the suppression ability of the metallocenes is difficult to evaluate by the method. In addition, even $FeCp_2$ having the highest vapor pressure among the metallocenes tested has a very low vapor pressure of 2.5 Pa (at 308 K: boiling point of n-pentane) [23]. Hence, it is difficult to control the amount of the added metallocene vapor to flame. This study employed the pool fire method, which involves measuring burning rate of the metallocene solution in n-pentane. Although this method cannot precisely control the amount of the metallocene added to the flame, heat from the flame formed over the fuel surface enables the addition of the metallocene vapor into the flame.

Measurement of burning rates of the fuel can provide clues to characterization of the pool fire. This experiment was conducted to evaluate the flame suppression effect of the metallocene in the gas phase. As mentioned above, this study employed n-pentane as a fuel because of relatively higher solubility of the metallocenes in n-pentane.

The water-insoluble metallocene used in this study should be added to the air in powder form. However, this method makes it very difficult to simply evaluate the metallocene for fire extinguishing effect because it depends strongly on not only their radical recombination effect but also physical effects including particle size. In this study, the metallocene, was added to the fuel in a way that eliminates the physical effects.

First the burning rate of the fuel was measured. As a result, the burning rate increased gradually with time, and approached a plateau of 2.7 mm min^{-1}. The value was used as a reference value.

The experiment confirmed that the burning rate decreased with an increase in the concentration of the metallocene over the concentration range of the measurement (10–200 ppm), i.e., the burning rates of all the solutions reached a minimum at 200 ppm. As mentioned above, the present study does not examine the solution with the metallocene concentration of more than 200 ppm for the burning rate. The reason is that saturation concentration of $MnCp_2$ is 200 ppm.

At 200 ppm, assuming that the metallocene and n-pentane are added into the flame as keeping the same ratio, the mole fractions of the maximum total metallic species in gas phase are 2.03×10^{-6} (Cr), 1.99×10^{-6} (Mn), 1.98×10^{-6} (Fe), 1.95×10^{-6} (Co), and 1.95×10^{-6} (Ni). There is no significant difference in the mole fractions among the metallocenes. Since the flame suppression effectiveness depends strongly on a mole fraction of the inhibiting species in gas phase at the flame, estimation of the mole fraction is of great importance for evaluating their suppression effectiveness and the ranking of the metals' suppression ability. However, we do not refer to their accurate mole fractions in the gas phase here because the metallocene concentration in the fuel was used in this study. This is because the metallocene was added not to the flame but the fuel, and a small amount of the metallocene remained at the bottom of the pan when the fuel was burned out.

The normalized burning rates of the solution (200 ppm) are illustrated in Fig. 9. The normalized

burning rates of $NiCp_2/n$-pentane, $CoCp_2/n$-pentane, $FeCp_2/n$-pentane, $MnCp_2/n$-pentane, and $CrCp_2/n$-pentane were determined to be 0.91, 0.85, 0.76, 0.53, and 0.08, respectively, i.e., the normalized burning rates of all the solutions are clearly less than 1. In particular, $CrCp_2$ showed the significant ability to decrease the burning rate. In addition, as can be seen from Fig. 9, the normalized burning rate is in order of $NiCp_2 > CoCp_2 > FeCp_2 > MnCp_2 > CrCp_2$, showing that the metallocenes are arranged in order of the atomic number of their central metal.

4. Discussion

The filter paper fire experiment revealed that $FeCp_2$, for example, had the strong inhibition effect in lower concentrations; in contrast, it had no effect of decreasing the flame spread rate in higher concentrations. It is known that the inhibiting iron species are FeO, FeOH, and $Fe(OH)_2$ [5, 10]. The inhibiting species in excess of the super-equilibrium concentration are effective in the recombination of radicals in gas phase. Although the suppression effectiveness can vary with flame type, in general, the effective flame suppression is not observed at higher concentrations [15]. Note that the concentration used in our study is not concentration in the flame but one in the specimen. Although the metallocene concentration (or mole fraction) in the flame cannot be described, the metallocene used in our experiments showed the same concentration dependency.

The pool fire experiments showed that all the metallocenes led to a decrease in the burning rate.

From a macroscopic viewpoint, the fuel temperature near the fuel surface is lower than the degradation point of the metallocene as shown in Section 3.2, suggesting that the metallocene does not decompose in the liquid phase. Hence, these metallocenes probably exhibit the flame suppression effect in the gas phase. The suppression effect can be governed by the following factor(s): (i) vapor pressure of the fuel; (ii) vapor pressure of the metallocene; (iii) the ease of the metallocene degradation in the gas phase; and (iv) the suppression ability of the transition-metal species formed from the metallocene.

With respect to the factor (i), the dissolved metallocene can decrease vapor pressure of the fuel, thereby reducing amount of the fuel vapor into the flame. Each solution used in this study, however, had a same molality in this experiment, and vapor pressure of the fuel mainly depends on the molality (mol kg^{-1}). Hence, the influence of each metallocene on the vapor pressure of the fuel was the same; in addition, the molalities are so small that this influence can be neglected.

Although there was little difference among the onset temperatures obtained from TG measurements (see Table 2), the ease regarding factor (iii) can be explained by the order of the onset temperature because the order of decreasing the normalized burning rates was in excellent agreement with the order of decreasing the onset temperature. For some metallocenes, enthalpies of disruption concerning metal−ligand bond have been studies by Swart [24]. Using density functional theory at OPBE/TZP level, the enthalpies of their spin ground states of $NiCp_2$, $CoCp_2$, $FeCp_2$, $MnCp_2$, and

CrCp$_2$ is calculated to be 701 kcal mol^{-1}, 676 kcal mol^{-1}, 658 kcal mol^{-1}, 576 kcal mol^{-1}, and 609

kcal mol^{-1}, respectively. Although the slightly anomalous order is observed, the disruption

enthalpies are arranged in order of the atomic number of their central metal, also supporting our

results. The difference among the enthalpies is relatively large in flame.

With respect to factor (iv), the suppression effectiveness varies with the metal species [26]. In all

the experiments (except the TG experiment), CrCp$_2$, MnCp$_2$, and FeCp$_2$ had a strong suppression

effect, and the order was in excellent agreement with the atomic number of their central metal. The

order can be accounted for by the fact that the flame suppression effect of suppression species

containing Cr are stronger than that of inhibition species containing Mn [25], and manganese species

offers higher vapor pressures than iron ones [2]. The information on catalytic effect of metals on

radical recombination was summarized by Linteris et al. [15], and their ranking of the metallic

inhibitors is nearly same as the order obtained in this work (Cr > Mn > Fe > Co > Ni). It should be

noted that there is a slight difference in the flame suppression ability. The suppression effectiveness

of Mn- and Fe-containing compounds was studied by Linteris et al [2]. Using a premixed CH$_4$/O$_2$/N$_2$

flame with methylcyclopentadienyl manganese tricarbonyl and Fe(CO)$_5$, the study provided detailed

information concerning their inhibition mechanism: there were similarities between the mechanisms

of the Mn- and Fe-containing compounds; in addition, a mole fraction of Mn(OH)$_2$, which is the

most important inhibiting species, decreased steeply at high temperatures ($T > 1800$ K). As a result,

they concluded that Mn was less effective than Fe. Conversely, the present study confirmed that Mn was more effective than Fe. Since the flame temperatures in this study were not so high [27], this is attributed to the difference in their flame temperatures.

Since the metallocene was not added directly to the flame in this study, their concentrations in the flame were unknown. Hence, this experiment may provide only qualitative information on the comparative suppression effect of the metallocenes. However, since the counterions of the metallocenes are identical, direct comparison of the suppression effect among the metals can be made.

Hence, the suppression ability is probably dominated by these factors. The factors influence the flame, reducing heat from flame to the fuel surface and lowering the burning rate. However, the extent to which these factors influence the flame suppression remains an arguable issue.

5. Conclusions

The flame suppression abilities of the metallocenes ($NiCp_2$, $CoCp_2$, $FeCp_2$, $MnCp_2$, and $CrCp_2$) were experimentally evaluated by combusting filter paper on which the metallocene was absorbed, by thermogravimetric analysis for metallocene/cellulose specimens, and by burning a solution of metallocene in n-pentane.

The first experiment (the filter paper fires) reveals that the extinction limits of $FeCp_2$, $MnCp_2$,

and $CrCp_2$ are smaller by a factor of 11, 35, 75, respectively, compared to $NH_4H_2PO_4$, which is a conventional multipurpose extinguishing agent.

The second experiment (the TG experiment) confirms that there are no obvious differences in activation energies regarding degradation of cellulose, indicating that the metallocenes does not exhibit the flame suppression ability in the solid phase.

The third experiment (the pool fires) shows that: (i) all the metallocenes remarkably decrease the burning rate of the fuel even in their lower concentrations; (ii) the phase in which the suppression effect is exhibited can be in gas phase; and (iii) the normalized burning rate is in order of $NiCp_2 > CoCp_2 > FeCp_2 > MnCp_2 > CrCp_2$.

Finally we conclude that the flame suppression ability of the metallocene is in order of $CrCp_2 > MnCp_2 > FeCp_2 > CoCp_2 > NiCp_2$, i.e., the metallocenes are arranged in order of the atomic number of their central metal. Although the metallocenes have a problem regarding long-term storage, these metallocenes used in this study are expected to be excellent flame suppressants. Moreover, our experiments can provide a clue to the development of a novel fire-extinguishing agent.

References

[1] X. Ni, K. Kuang, D. Yang, X. Jin, G. Liao, A new type of fire suppressant powder of $NaHCO_3$/zeolite nanocomposites with core–shell structure, Fire Safety J. 44 (2009) 968–975.

[2] G.T. Linteris, V.D. Knyazev, V.I. Babushok, Inhibition of premixed methane flames by manganese and tin compounds, Combust. Flame 129 (2002) 221–238.

[3] V. Babushok, W. Tsang, G.T. Linteris,, D. Reinelt, Chemical limits to flame inhibition, Combust. Flame 115 (1998) 551–560.

[4] W.A. Rosser, Jr, S.H. Inami, H. Wise, The effect of metal salts on premixed hydrocarbon-air flames, Combust. Flame 7 (1963) 107–119.

[5] I.E. Gerasimov, D.A. Knyazkov, A.G. Shmakov, A.A. Paletsky, V.M. Shvartsberg, T.A. Bolshova, O.P. Korobeinichev, Proc. Combust. Inst. 33 (2011) 2523–2529.

[6] B.A. Williams, J.W. Fleming, CF_3Br and other suppressants: differences in effects on flame structure, Proc. Combust. Inst. 29 (2002) 345–351.

[7] M.D. Rumminger, D. Reinelt, V. Babushok, G.T. Linteris, Numerical study of the inhibition of premixed and diffusion flames by iron pentacarbonyl, Combust. Flame 116 (1999) 207–219.

[8] D. Reinelt, G.T. Linteris, Experimental study of the inhibition of premixed and diffusion flames by iron flames by iron pentacarbonyl, 26th Symp. (Int.) Combust. (1996) 1421–1428.

[9] U. Bonne, W. Jost, H.G. Wagner, Iron pentacarbonyl in methane-oxygen (or air) flames, Fire Res. Abstr. Rev. 4 (1962) 6–18.

[10] G.T. Linteris, M.D. Rumminger, V. Babushok, W. Tsang, Flame inhibition by ferrocene and blends of inert and catalytic agents, Proc. Combust. Inst. 28 (2000) 2965–2972.

[11] J. Zhang, C.M. Megaridis, Soot suppression by ferrocene in laminar ethylene/air nonpremixed flames, Combust. Flame 105 (1996) 528–540.

[12] J.B.A. Mitchell, Smoke reduction from burning crude oil using ferrocene and its derivatives, Combust. Flame 86 (1991) 179–184.

[13] P. Carty, J. Grant, A. Simpson, Synthesis of a novel ferrocene derivative having flame−retardant and smoke−suppressant properties, Appl. Organomet. Chem. 2 (1988) 277–280.

[14] M.M. Hirschler, Soot from fires: III. soot suppression, J. Fire Sci. 42 (1986) 42–72.

[15] G.T. Linteris, M.D. Rumminger, V.I. Babushok, Catalytic inhibition of laminar flames by transition metal compounds, Prog. Ener. Combust. Sci. 34 (2008) 288–329.

[16] V. Babushok, W. Tsang, Inhibitor rankings for alkane combustion, Combust. Flame 123 (2000) 488–506.

[17] Y. Koshiba, H. Ohtani, Experimental study of fire-extinguishing agents for throwing fire extinguishers, Shoken Shuho 63 (2010) 152–158.

[18] Japan Association for Fire Science and Engineering, Kasai Binran (Fire handbook), Kyoritsu Publishers, Tokyo, Japan (1997).

[19] H.E. Kissinger, Reaction kinetics in differential thermal analysis. Anal. Chem. 29 (1957) 1702–1706.

[20] D. Jelić, B.T. Tomić, S. Mentus, A kinetic study of copper(II) oxide powder reduction with

hydrogen, based on thermogravimetry, Thermochim. Acta 521 (2011) 211–217.

[21] S. Chen, H. Yu, W. Ren, Y. Zhang, Thermal degradation behavior of hydrogenated

nitrile−butadiene rubber (HNBR)/clay nanocomposite and HNBR/clay/carbon nanotubes

nanocomposites, Thermochim. Acta 491 (2009) 103–108.

[22] H. Ohtani, T. Hirakura, Y. Uehara, Fire extinguishments by metal of ammonium salts, Combust.

Sci. Technol. 7 (2000) 241–248.

[23] V.N. Emel'yanenko, S.P. Verevkin, O.V. Krol, R.M. Varushchenko, N.V. Chelovskaya, Vapour

pressures and enthalpies of vaporization of a series of the ferrocene derivatives, J. Chem.

Thermodyn. 39 (2007) 594–601.

[24] M. Swart, Metal−ligand bonding in metallocenes: Differentiation between spin state,

electrostatic and covalent bonding, Inorg. Chim. Acta 360 (2007) 179−189.

[25] E.M. Bulewicz, P.J. Padley, D.H. Cotton, D.R. Jenkins, Metal-additive-catalysed

radical-recombination rates in flames, Chem. Phys. Lett. 9 (1971) 467−468.

[26] G.T. Linteris, V.R. Katta, F. Takahashi, Experimental and numerical evaluation of metallic

compounds for suppressing cup-burner flames, Combust. Flame 138 (2004) 78−96.

[27] T. Hirano, S.E. Norekis, T.E. Waterman, Combust. Flame 23 (1974) 83-96.

Figure captions

Fig. 1 Chemical structures of ferrocene, manganocene, nickelocene, chromocene, and cobaltocene.

Fig. 2 Schematic diagram of experimental apparatus for the filter paper fire.

Fig. 3 Schematic diagram of experimental apparatus for the pool fire.

Fig. 4 Normalized flame spread rate *vs*. concentration of the flame suppressant: (a) Ammonium dihydrogen phosphate. (b) Nickelocene. (c) Cobaltocene. (d) Ferrocene. (e) Manganocene. (f) Chromocene. Circles: combustion with flame; triangles: glowing; squares: extinction. The insets of Fig. 4d, e and f show the zoomed in portion of the data.

Fig. 5 Normalized flame spread rate plotted as a function of the storage time (○: flame suppressant is manganocene; □: flame suppressant is chromocene). (a) The stored specimens in humid air under light shielding condition. (b) The stored specimens in dry air under light shielding condition.

Fig. 6 TG (○) and DTG (▲) curves of manganocene.

Fig. 7 TG (○) and DTG (▲) curves of the manganocene/cellulose specimen (concentration of $MnCp_2$ in cellulose specimen is set to 1.50×10^{-5} mol g^{-1}).

Fig. 8 Kissinger plot of the manganocene/cellulose specimen for activation energy determination.

Fig. 9 The normalized burning rate of the solution of the metallocene in *n*-pentane at a concentration

of 200 ppm.

Table captions

Table 1 Absorption limits of the filter paper, initiation concentrations of glowing, and extinction

limits.

Table 2 Temperatures at onset ($T_{onset, M}$) and peak ($T_{max, M}$), and residual mass at 873 K of the

metallocene (RM_M) ($\beta = 5$ K min^{-1}).

Table 3 Temperatures at onset ($T_{onset, c}$) and peak ($T_{max, c}$), and residual mass at 873 K of the

metallocene/cellulose specimen (RM_c) ($\beta = 5$ K min^{-1}).

Table 4 Apparent activation energies relating to the degradation of cellulose determined by the

Kissinger method.

Table

Flame suppression agent	Absorption limit $(\times\ 10^{-4}\ \text{mol g}^{-1})$	Initiation concentration of glowing $(\times\ 10^{-4}\ \text{mol g}^{-1})$	Extinction limit $(\times\ 10^{-4}\ \text{mol g}^{-1})$
$NH_4H_2PO_4$	13.5	1.00	5.25
$NiCp_2$	6.50	ND[a]	ND[a]
$CoCp_2$	7.00	ND[a]	ND[a]
$FeCp_2$	11.00	0.10	0.50
$MnCp_2$	2.00	0.20	0.15
$CrCp_2$	3.50	0.20	0.07

[a] ND: not detected

Table 2

Metallocene	$T_{\text{onset, M}}$ (K)	$T_{\text{max, M}}$ (K)	RM_{M} (%)
NiCp$_2$	381	413	0.01
CoCp$_2$	378	412	0.02
FeCp$_2$	376	410	0.01
MnCp$_2$	375	409	0.01
CrCp$_2$	373	408	0.01

Table 3

Specimen	$T_{\text{onset, c}}$ (K)	$T_{\text{max, c}}$ (K)	RM_{c} (%)
NiCp$_2$/cellulose	603	632	2.6
CoCp$_2$/cellulose	606	635	2.7
FeCp$_2$/cellulose	603	631	2.7
MnCp$_2$/cellulose	600	629	2.4
CrCp$_2$/cellulose	608	630	2.4
cellulose	603	633	2.1

Table 4

Specimen	Activation energy E_a (kJ mol^{-1})
NiCp$_2$/cellulose	347
CoCp$_2$/cellulose	349
FeCp$_2$/cellulose	346
MnCp$_2$/cellulose	345
CrCp$_2$/cellulose	347
cellulose	348

Figure 1
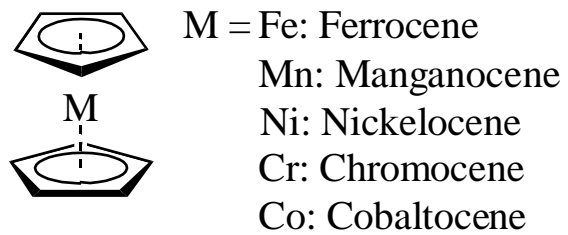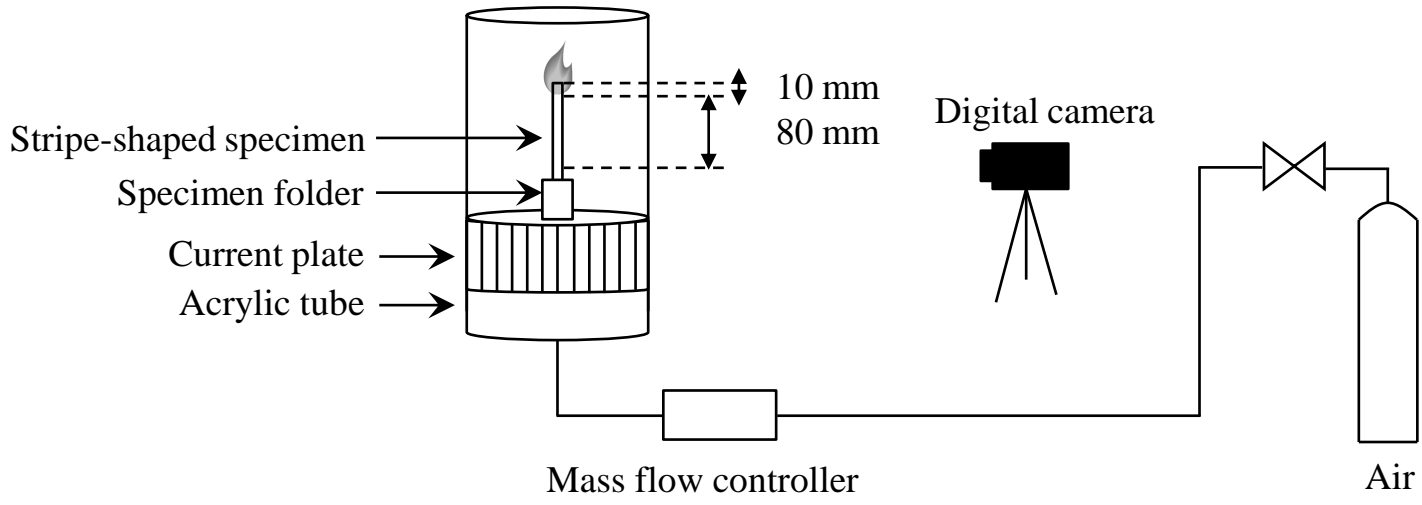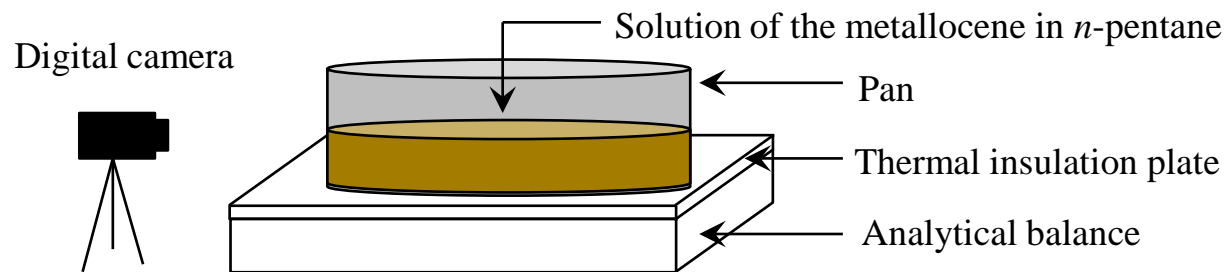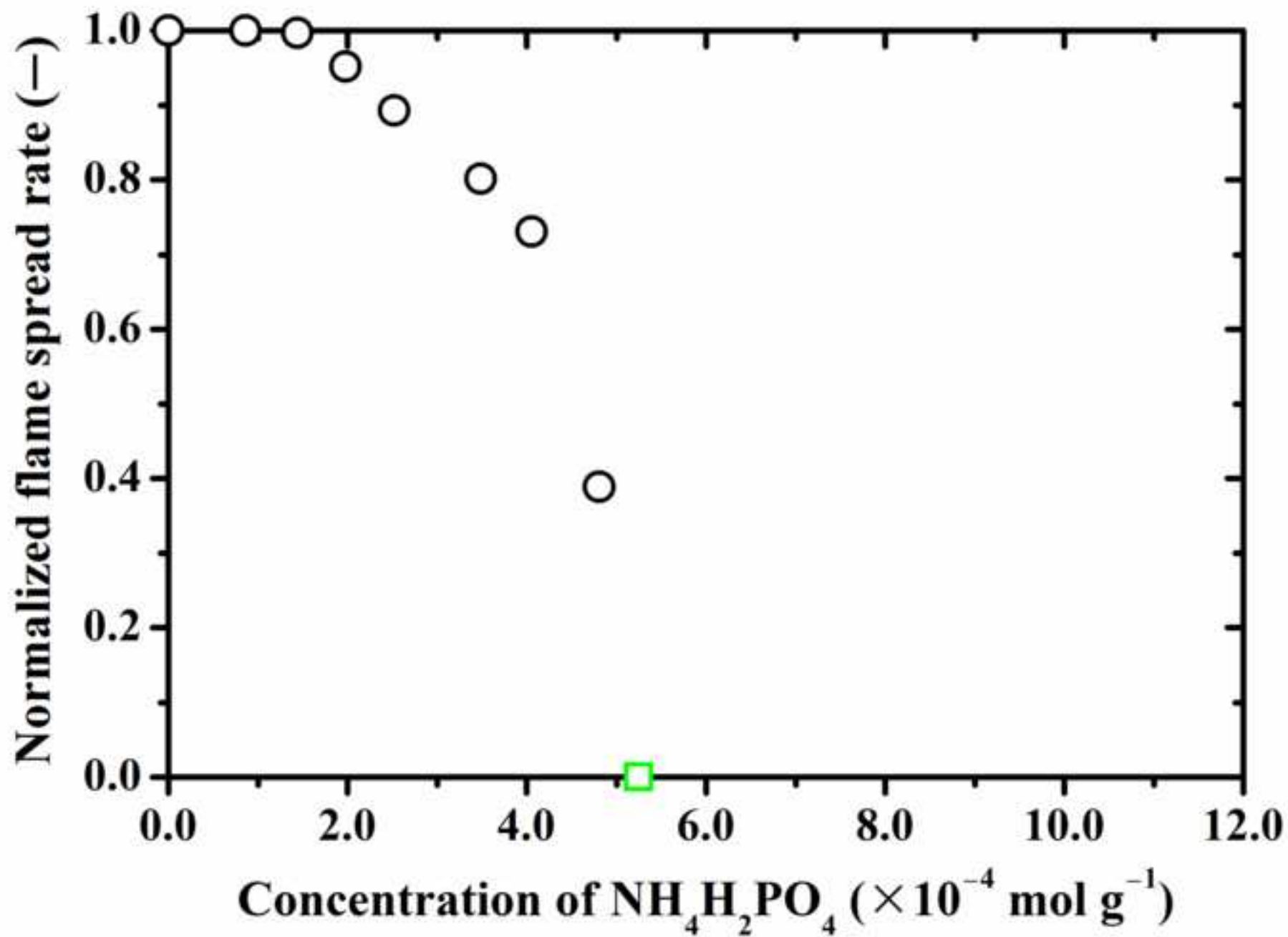
M = Fe: Ferrocene
Mn: Manganocene
Ni: Nickelocene
Cr: Chromocene
Co: Cobaltocene

Figure 2

Stripe-shaped specimen

Specimen folder

Current plate

Acrylic tube

10 mm
80 mm

Digital camera

Mass flow controller

Air

Figure 3

Digital camera

Solution of the metallocene in *n*-pentane

Pan

Thermal insulation plate

Analytical balance

Figure 4a: Normalized flame spread rate (−) versus Concentration of $NH_4H_2PO_4$ ($\times 10^{-4}$ mol g^{-1})
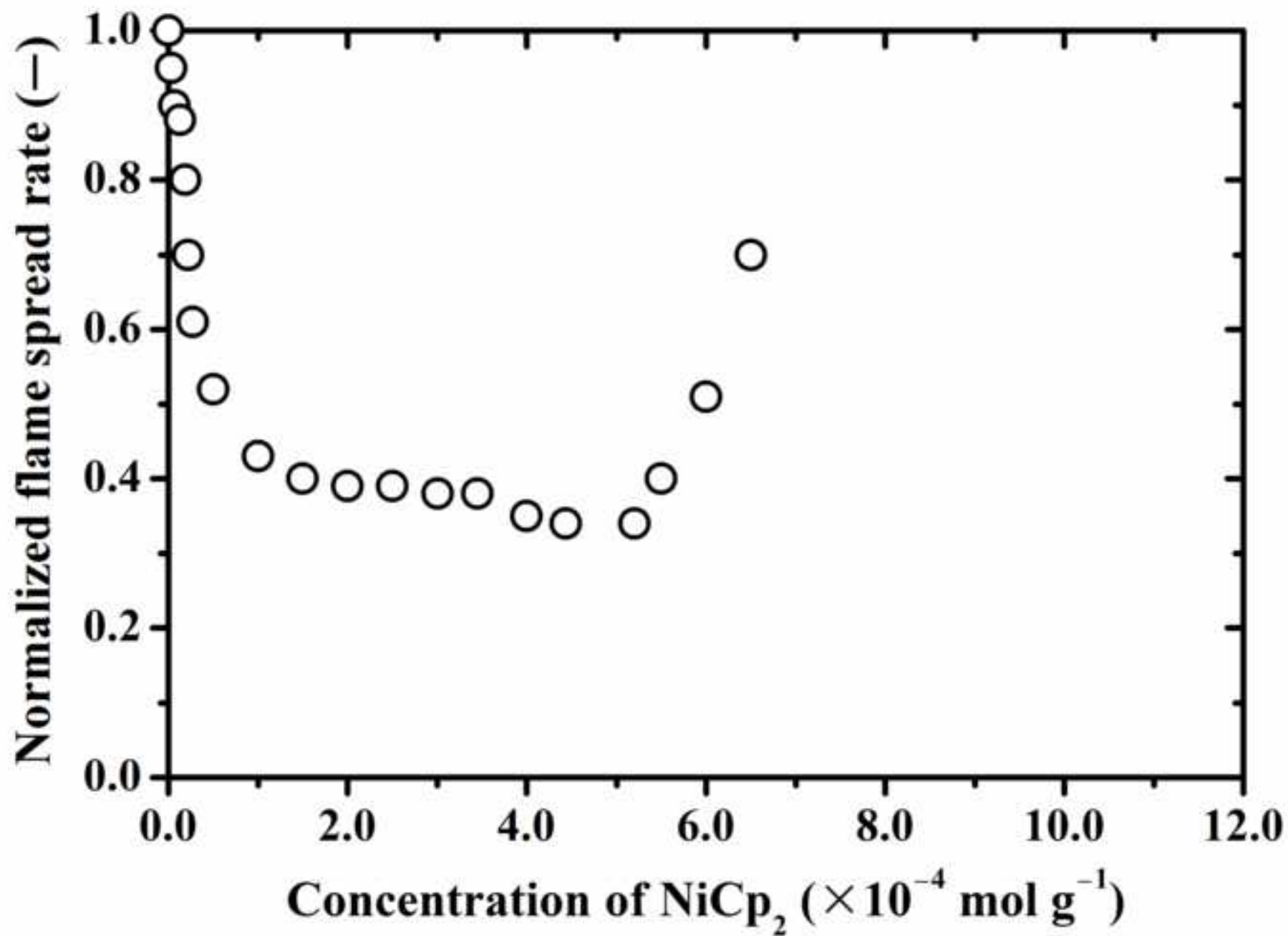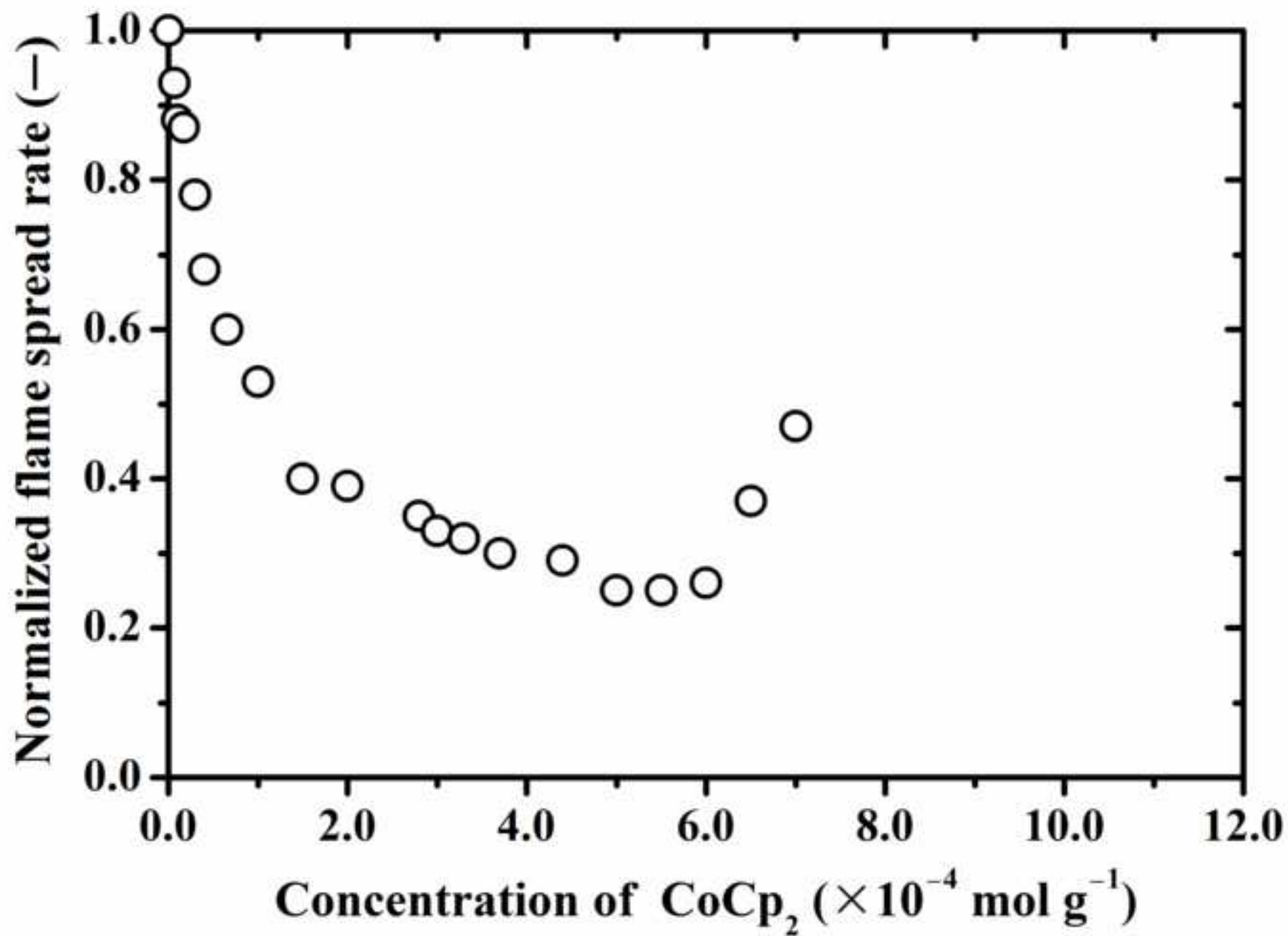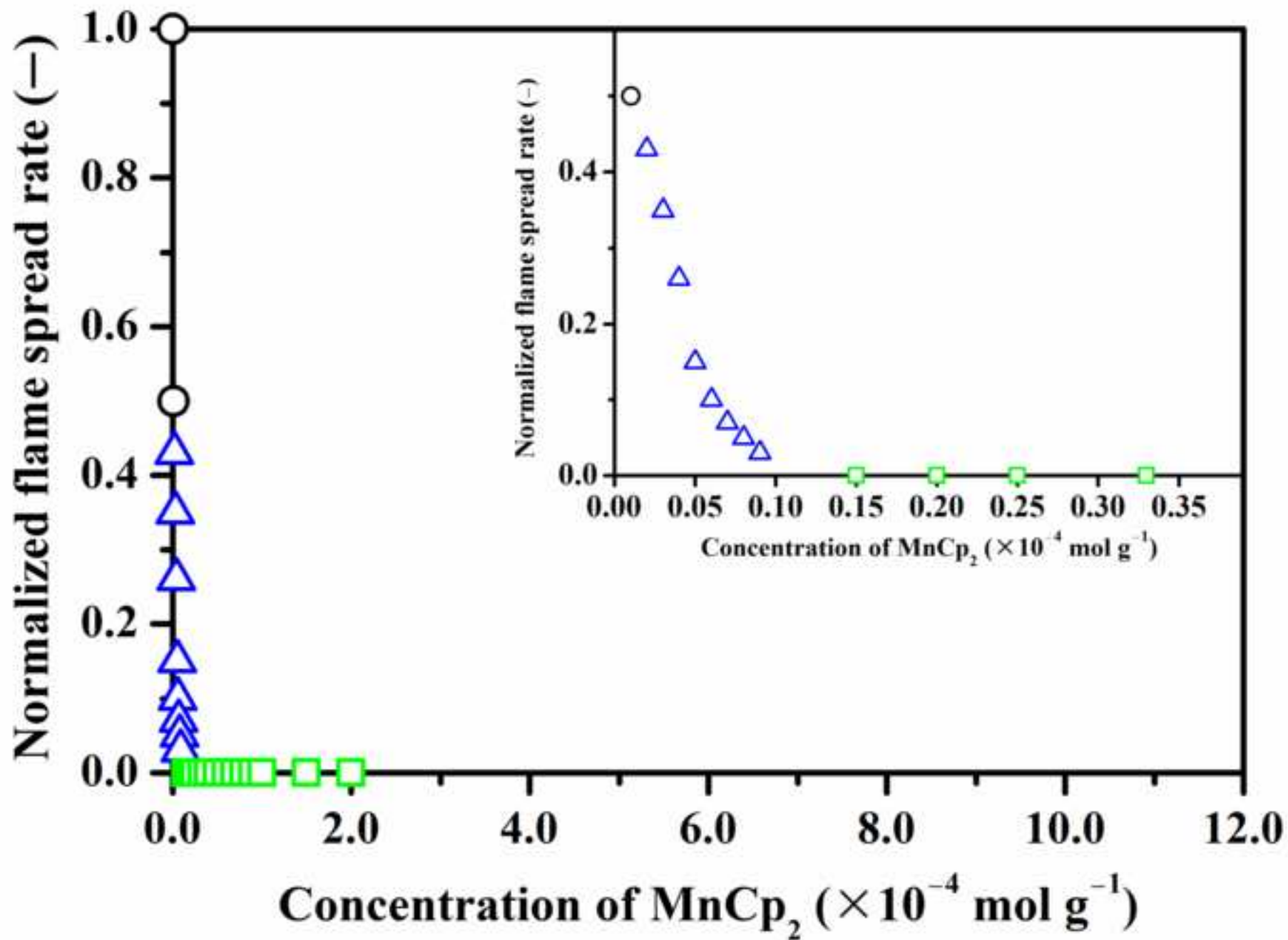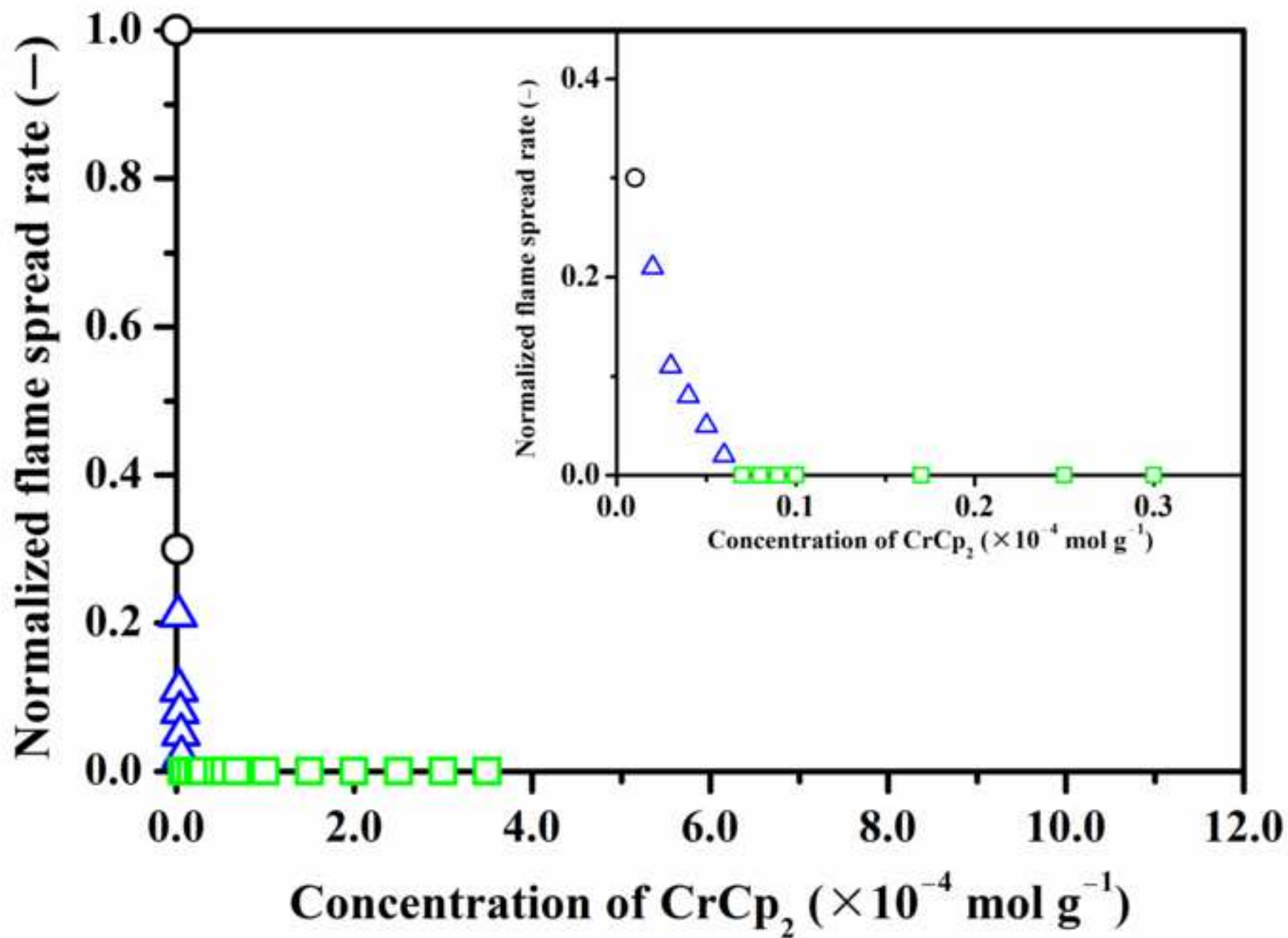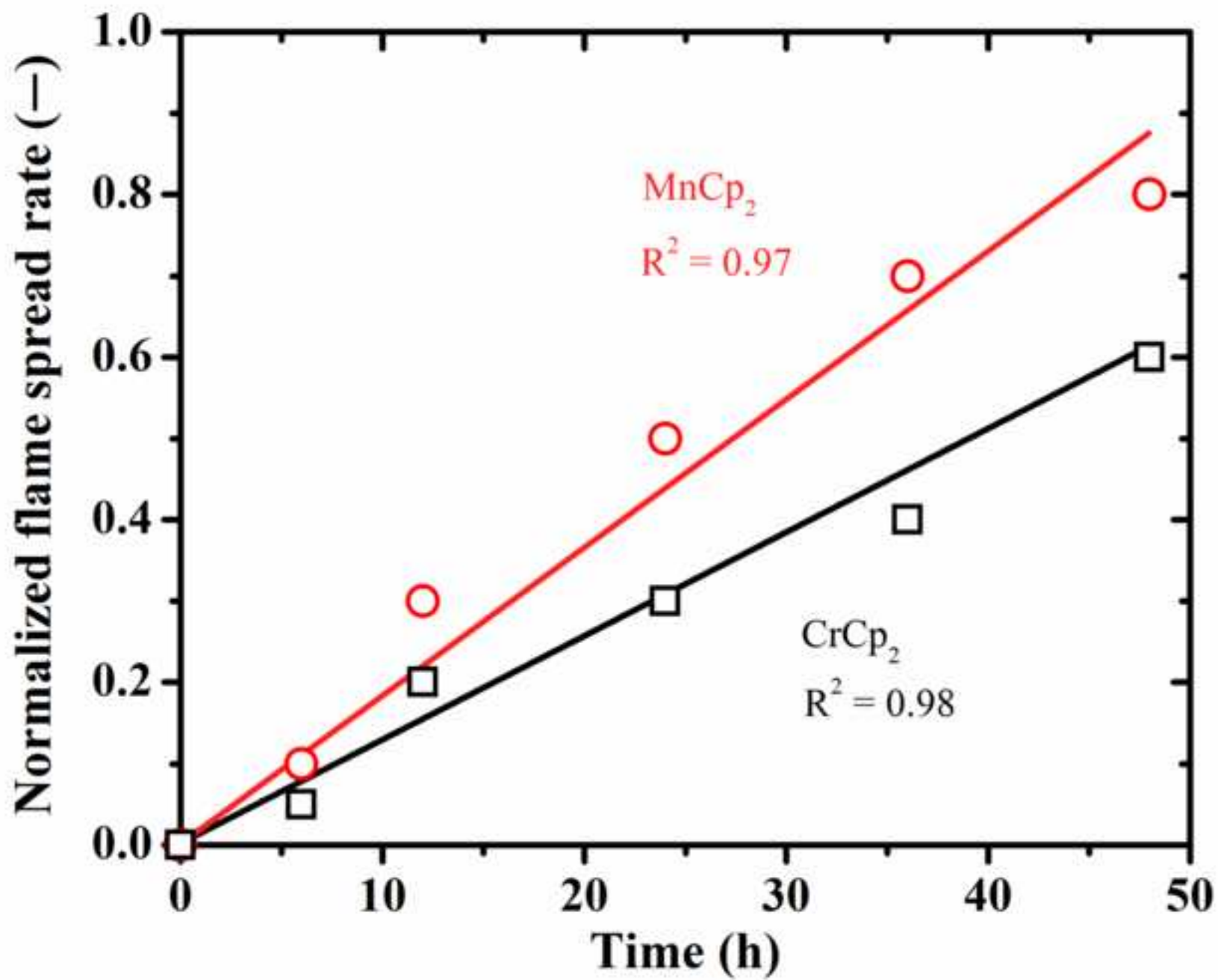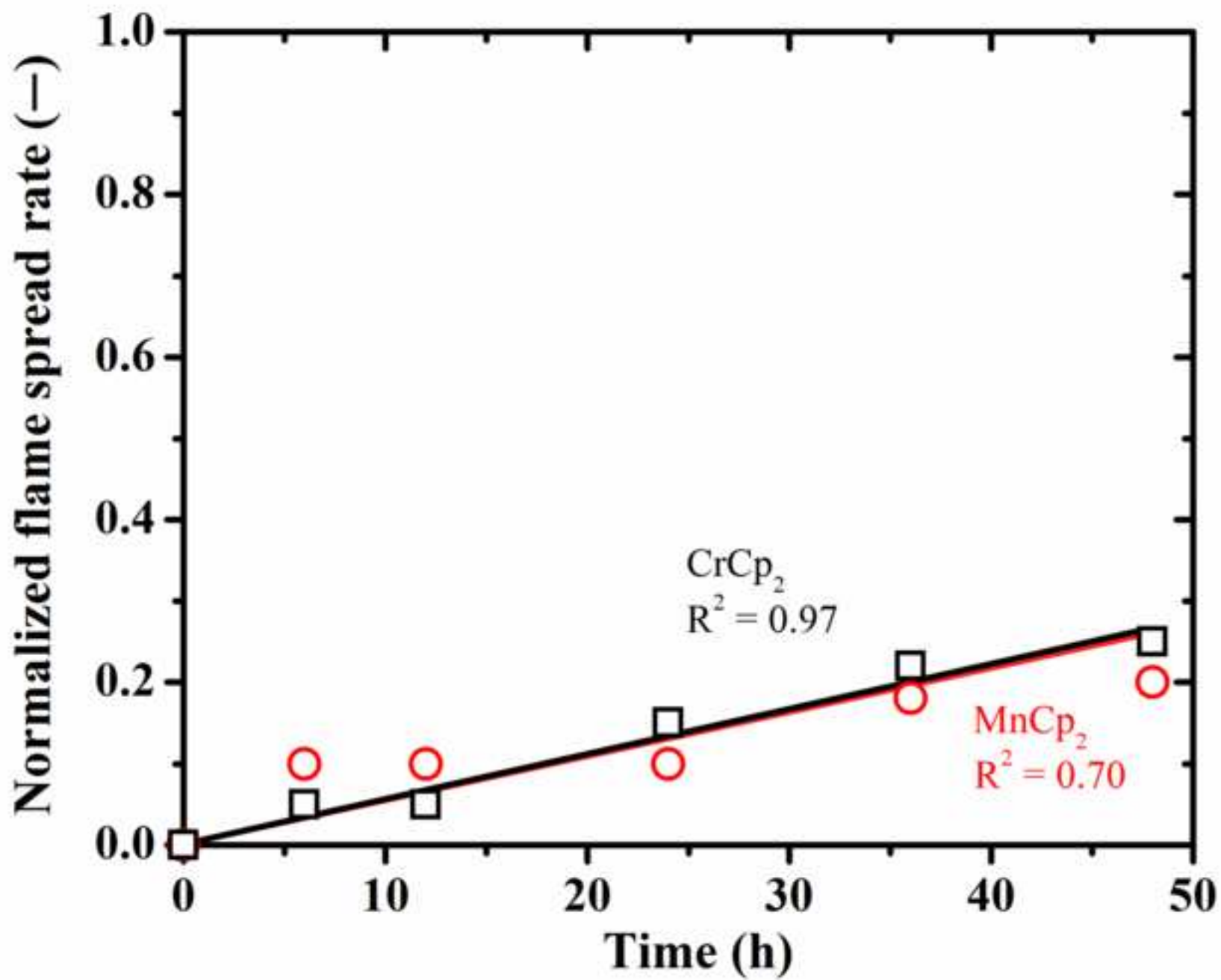
Figure 4b

Figure 5b

Figure 6
Click here to download high resolution image
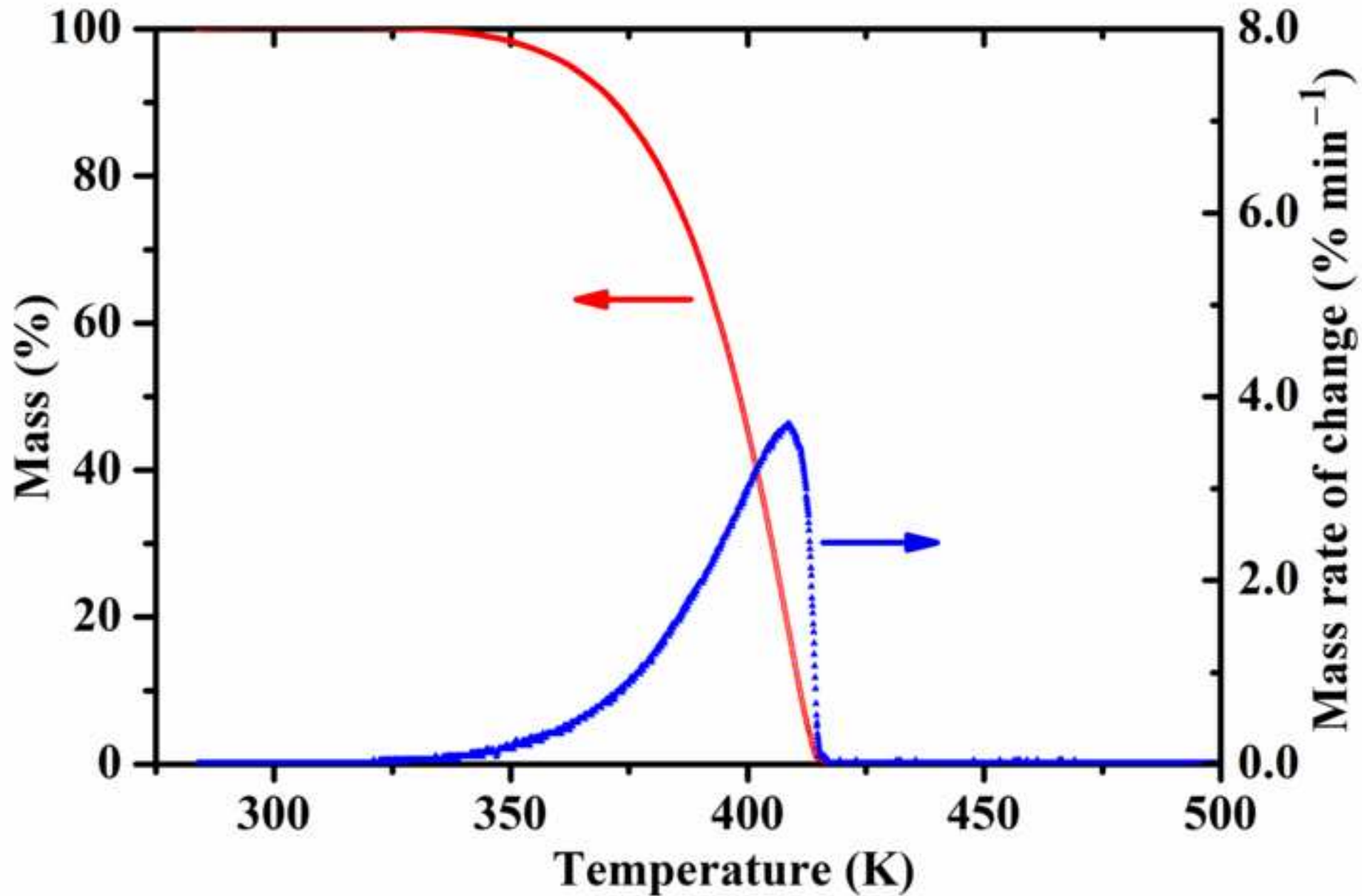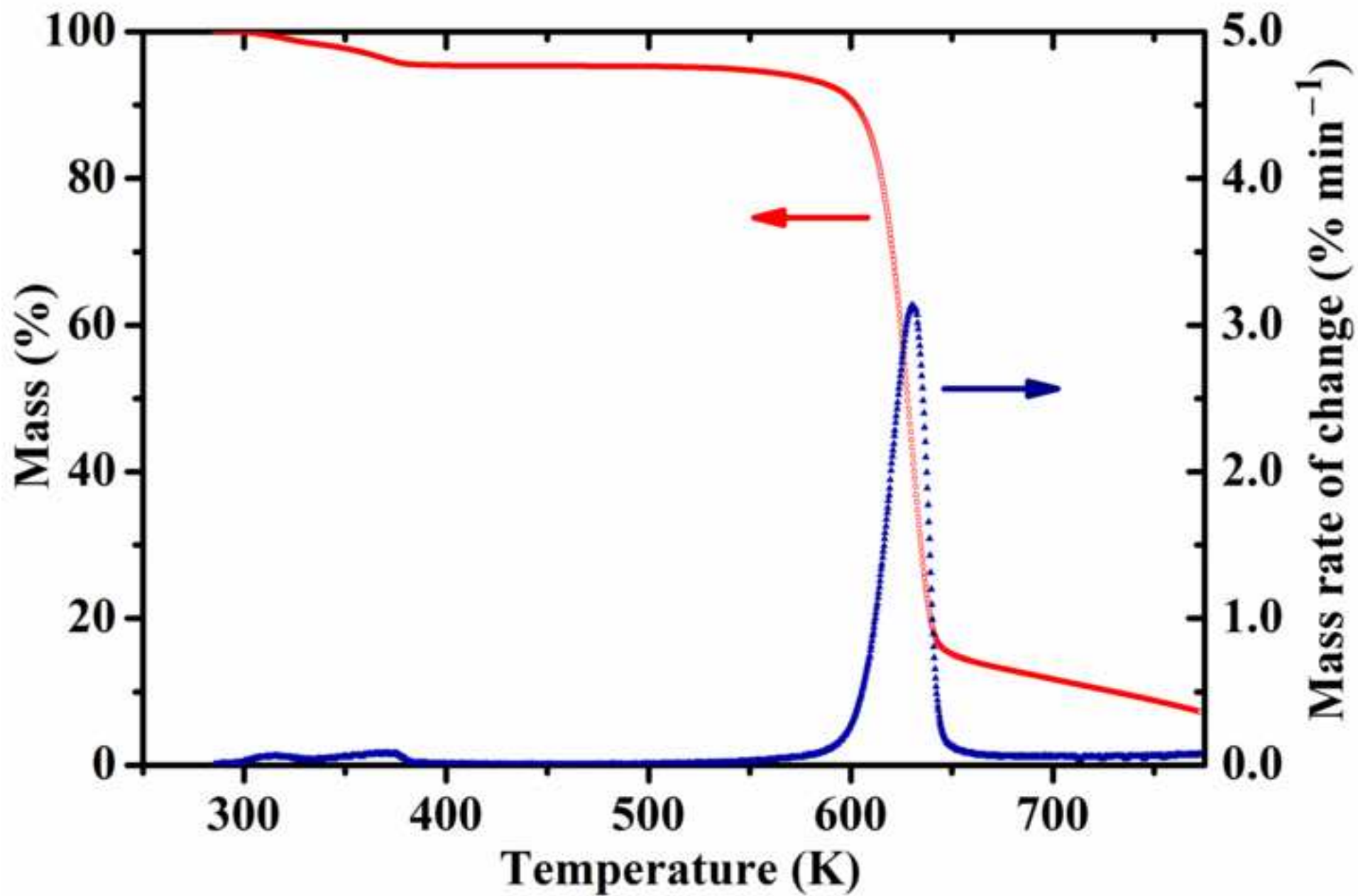
Figure 8
Click here to download high resolution image
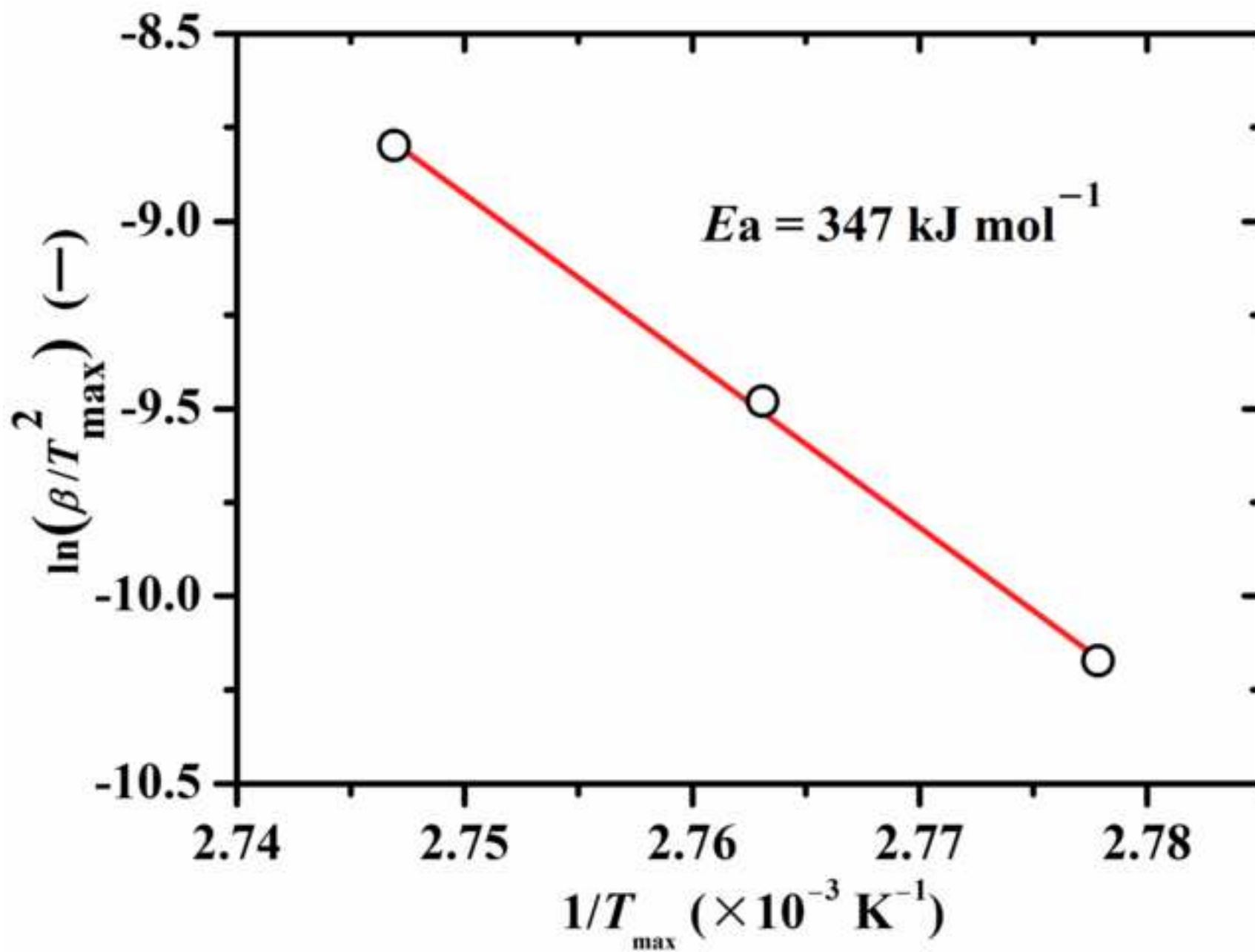
Figure 8

Figure 9
Click here to download high resolution image
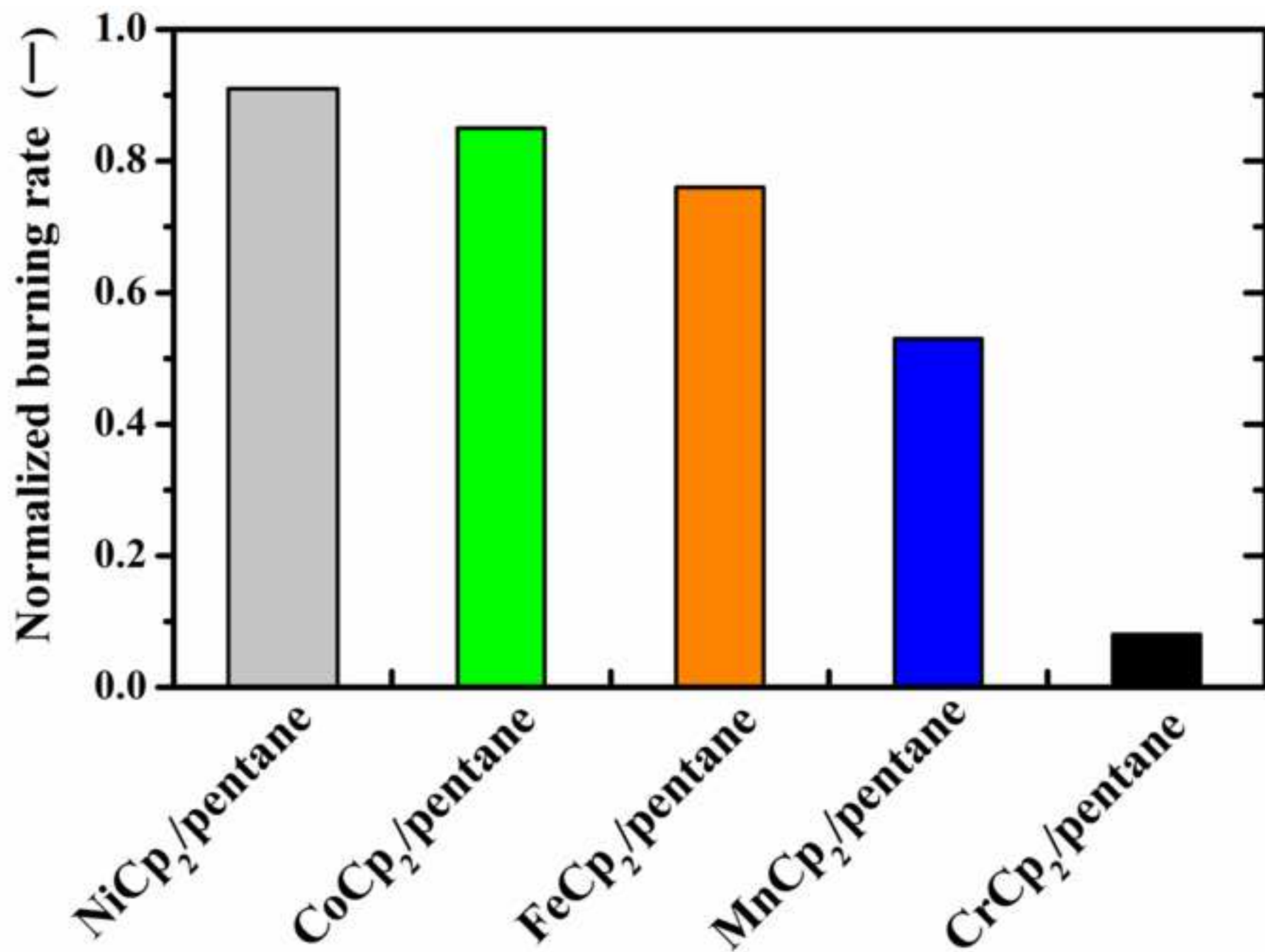
Highlights

We experimentally investigate metallocenes for flame suppression ability.

Metallocenes exhibit the better flame suppression ability compared to $NH_4H_2PO_4$.

The order of the suppression ability is $CrCp_2 > MnCp_2 > FeCp_2 > CoCp_2 > NiCp_2$.